ACS Catalysis

Research Article

pubs.acs.org/acscatalysis

Brønsted–Evans–Polanyi and Transition State Scaling Relations of Furan Derivatives on Pd(111) and Their Relation to Those of Small Molecules

Shengguang Wang, Vassili Vorotnikov, Jonathan E. Sutton, and Dionisios G. Vlachos*

Department of Chemical and Biomolecular Engineering, Catalysis Center for Energy Innovation, and Center for Catalytic Science and Technology, University of Delaware, Newark, Delaware 19716, United States

Supporting Information

ABSTRACT: Brønsted–Evans–Polanyi (BEP) and transition state scaling (TSS) linear free energy relations are extended to C–H, O–H, C–O and C–C bond breaking reactions occurring on the ring and the functional groups of furan (hydrofuran, dihydrofuran, trihydrofuran, and tetrahydrofuran) and furfural derivatives (e.g., furfural, furfuryl alcohol, methyl furan, etc.) on Pd(111). The relations perform statistically as well as those for small molecules reported previously. Hydrogenation/dehydrogenation reactions have smaller deviations compared to C–C and C–O bond breaking ones. This is in line with the degree of structural change during reaction and agrees with observations in previous works. We conclude that BEP relations developed for small molecules are not statistically different from those developed for furanics. A universal BEP relation is not statistically different from most of the BEP relations developed for furanics, with the exception of C–O, O–H and C–H scission reactions at the functional group, for which only the intercept is statistically different. Small-molecule BEP relations perform adequately for exploring biomass-relevant chemical kinetics on metal surfaces with higher accuracy than the universal BEP relation but lower accuracy than the BEPs of furanics. Finally, we make general observations about the effect of structural change and reaction energy on the accuracy of linear free energy relations on metal surfaces.

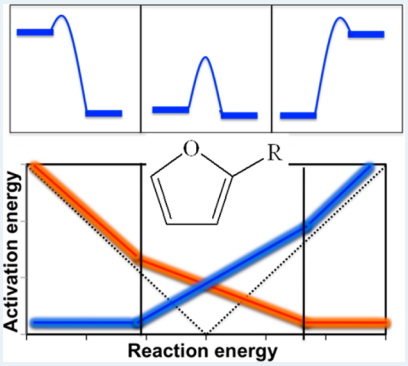

KEYWORDS: *furan derivatives, BEP, DFT, biomass chemistry, transition states, PBE-D3*

INTRODUCTION

The use of density functional theory (DFT) has become standard in computational catalysis over the past decade. Such calculations are typically performed to understand experimental findings, elucidate reaction mechanisms, build microkinetic models, and predict structure–property relations. However, we are faced with a combinatorial challenge when dealing with large reaction networks, especially those involving biomass derivatives.[1−3] To lessen the computational burden, linear correlations have been proposed to quickly estimate reaction barriers.[4−10]

$$E_a = \alpha \Delta E + \beta \quad (1)$$

$$E_{TS} = \alpha \Delta E_{FS} + \beta \quad (2)$$

Brønsted–Evans–Polanyi (BEP) relations (eq 1) were initially proposed for homogeneous chemistry by Brønsted, Bell, Evans and Polanyi.[11,12,4] One of the first applications of BEP relations to heterogeneous catalysis was by Pallassana and Neurock, who correlated the activation energies (E_a) of ethyl and ethylene species on pseudomophic Pd overlayers with the corresponding heats of reaction (ΔE) in exactly the same fashion as the traditional BEP correlations.[5,13] Liu and Hu were among the first to investigate the relationship of the transition state structure and the BEP correlation for heterogeneous catalysis.[14] Shortly after, Alcala et al. proposed an alternate BEP form correlating the transition state energy (E_{TS}) with the final state energy (E_{FS}).[15] This has recently been referred to as a transition state scaling (TSS) correlation (eq 2).[16] BEP and TSS relations have been extended to multifunctional reactants (acrolein).[17]

The common feature of the BEP and the TSS is the correlation of kinetics with thermodynamics of a chemical reaction. BEP relations directly correlate the activation energy with thermodynamic quantities, specifically the reaction energy, and can be derived from the transition state (TS) energy and final or initial state (FS or IS) energy from TSS relations.[10] BEP and TSS relations have been utilized to rapidly develop microkinetic models using limited data obtained from DFT-based electronic structure methods.[18−23] Today, BEP and TSS relations have been established for many reactions of molecular size usually up to two carbons[24,25,10] and have been utilized in many catalytic reactions.[26−28]

With recent political and economic pushes to convert biomass to chemicals and fuels, biomass pyrolysis has attracted much attention. Furanic (F) molecules make up a large fraction of byproducts in biomass pyrolysis and can be further

Received: October 17, 2013
Revised: December 8, 2013
Published: January 8, 2014

transformed into fuels and chemicals. However, there is limited scientific knowhow of such catalytic processes, and most of the elementary reactions are difficult or impossible to study using only experimental methods. Obtaining kinetic parameters for these reactions has only recently been investigated computationally.[29−31] However, there are currently no extensions of BEP and TSS relations to furan derivatives. In this paper, we extend BEP and TSS relations to reactions encountered in the upgrade of furanics on Pd(111). Similar to earlier work on small molecules, such relations could potentially be applied also to monolayer bimetallics[32] and can help accelerate the discovery of novel catalysts for biomass processing.

In conjunction with extending the linear free energy relations to furanic species, we are interested in understanding how free energy relations for furanic and small species compare in accuracy and universality (i.e., can correlations for small species be applied to furanics and vice versa) and the physical source of the homologous series classifications and resulting correlation error. We answer these two questions in four sections. First, we introduce the model system and investigate the accuracy of the universal free energy relations. Then we examine some possible definitions for homologous series based on molecular structure (e.g., functional group, species type, and binding modes) and bond type. Subsequently, we discuss the effect of molecular structure and reaction energy on correlation accuracy. Finally, we compare the general accuracy of the different homologous series and the possible implications of using small molecule correlations for estimating activation energies for furanic species. We close with a summary.

METHODS AND MODELS

For reactions of furan derivatives, we carried out plane-wave DFT calculations using the Vienna ab initio simulation package (VASP),[33,34] version 5.2.12. The electron−electron exchange and correlation energies were computed using the Perdew, Burke, and Ernzerhof functional with the latest dispersion correction, PBE-D3.[35,36] The projector augmented-wave method was used for the electron−ion interactions.[37,38] We used a plane-wave basis set with an energy cutoff of 400 eV. For bulk calculations, a tetrahedron method with Blochl corrections and 15 × 15 × 15 Monkhorst−Pack k-point mesh was used.[39,40] The optimized Pd fcc lattice constant was calculated to be 3.95 Å using the PBE and 3.90 Å using the PBE-D3, both of which are in good agreement with the experimental value of 3.89 Å.[41] The metal slab was modeled as a 4 × 4 unit cell composed of four atomic layers. The bottom two layers were frozen while the top two were allowed to relax. The vacuum between the slabs was set at 20 Å to minimize the effect of interaction between them. The Brillouin zone was sampled with a 3 × 3 × 1 k-point grid. For accurate total energies, we used the Methfessel−Paxton method with a smearing parameter of 0.1. Surface relaxation was performed until all forces were smaller than 0.05 eV/Å. The supercell for all gas-phase calculations was chosen to be 20 × 20 × 20 Å. The transition states were located using the climbing nudged elastic band (cNEB) method.[42] The calculations were considered to be converged when all forces were smaller than 0.05 eV/Å. The transition states were confirmed by the presence of a unique imaginary frequency for selected reactions. The data of small species are from reference,[43] which were calculated with SIESTA.[44]

Overview and Universal Linear Free Energy Relations. Scheme 1 shows the furan derivatives calculated in this paper.

Scheme 1. Schematic Structure of Furan Derivatives

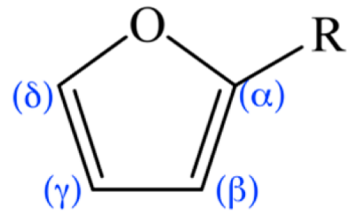

- The four carbon atoms are labeled as α, β, γ and δ.
- **R** denotes functional groups, including $-CH_2OH$, $-CHOH$, $-COH$, $-CH_2O$, $-CHO$, $-CO$, $-CH_3$, $-CH_2$, $-CH$, $-C$ and $-H$.

We analyzed 12 typical groups of 109 reactions including C−H, O−H, C−O and C−C bond scissions on furan ring, functional group and C2 molecules ($CH_xCH_yOH_z$, where x = 0−3, y = 0−2, z = 0−1). All reactions being discussed in this paper are listed in the Supporting Information together with reaction energies, activation energies, transition state energies and final state energies. The fitted BEP and TSS relations are listed in Table 1 together with the mean absolute error (AE), max AE, and 95% confidence intervals (CI). We point out that all BEP and TSS relations in this paper are in the dissociation direction. We also employed some data from our previous DFT study of furanics (furan and furfural) chemistry.[29,31]

It has been reported that for all the essential bond forming and bond breaking reactions, the reactivity of the metal surface correlates linearly with the reaction energy in a single universal relation.[16,24] Such correlations provide an easy way of establishing trends in reactivity among transition metals. Wang et al. reported universal BEP and TSS relations fitted for 249 dehydrogenation reactions (C−H, N−H, O−H scissions) on different transition metals, and the mean AE were 0.27 and 0.28 eV for universal BEP and TSS, respectively.[16] The mean AE of a universal TSS relation of C−C, C−O, C−N, N−O, N−N and O−O bond breaking on different transition metals was reported to be 0.35 eV.[24]

In Figure 1, we plot the universal BEP and TSS relations of all reactions on Pd(111) calculated herein. For the TSS relations in this paper, all of the energies of transition states and final states were referred to the gas-phase energies of CH_4, H_2 and H_2O (reported in the Supporting Information). The mean AE of BEP and TSS relations are both 0.34 eV in each case, as listed in Table 1. The scatter of the universal relations found here is close to those of small molecules reported previously (0.27, 0.28[16] and 0.35[24]). This indicates that BEP and TSS relations developed for furanics have comparable accuracy and can potentially be equally used in barrier estimation (see below).

The universal relations provide a fast and easy way to explore trends in catalytic reactions. However, the accuracy decreases when many types of reactions are grouped together. For example, the max AE of the universal BEP and TSS relations from all of our calculations is 1.57 and 1.71 eV, respectively. This indicates that when the universal relations are used to compute barriers, the worst results could have errors of about 1.5 eV. Higher accuracy correlations are usually required for

dx.doi.org/10.1021/cs400942u | ACS Catal. 2014, 4, 604−612

Table 1. BEP and TSS Relations of C−H, O−H, C−O and C−C Bond Scissions, Mean and Max Absolute Errors (AE) (in eV), Confidence Intervals (CI) of Slope and Intercept

reaction	points		relation	mean AE	max AE	CI slope	CI intercept
universal	109	BEP	$y = 0.83x + 1.14$	0.34	1.57	0.12	0.09
		TSS	$y = 0.97x + 1.26$	0.34	1.71	0.03	0.18
C−H scission							
(1) at furan ring	9	BEP	$y = 0.59x + 1.17$	0.11	0.20	0.20	0.12
		TSS	$y = 0.88x + 1.78$	0.16	0.44	0.17	0.77
(2) at functional group	5	BEP	$y = 0.51x + 0.70$	0.06	0.13	0.25	0.14
		TSS	$y = 0.92x + 1.42$	0.17	0.23	0.14	1.31
(3) small species	19	BEP	$y = 0.59x + 1.00$	0.15	0.35	0.32	0.17
		TSS	$y = 0.85x + 1.47$	0.17	0.46	0.20	0.39
combined C−H	33	BEP	$y = 0.51x + 0.98$	0.18	0.36	0.17	0.10
		TSS	$y = 0.93x + 1.38$	0.21	0.53	0.03	0.14
O−H scission							
(4) at functional group	6	BEP	$y = 0.71x + 0.71$	0.15	0.27	0.64	0.27
		TSS	$y = 0.59x + 3.46$	0.14	0.33	0.80	5.25
(5) small species	8	BEP	$y = 0.66x + 0.78$	0.07	0.22	0.27	0.11
		TSS	$y = 1.01x + 0.77$	0.12	0.38	0.33	0.81
combined O−H	14	BEP	$y = 0.70x + 0.75$	0.12	0.29	0.23	0.09
		TSS	$y = 0.99x + 0.82$	0.14	0.39	0.06	0.26
C−O scission							
(6) ring-opening	11	BEP	$y = 0.90x + 1.00$	0.45	0.98	0.90	0.55
		TSS	$y = 0.86x + 1.77$	0.33	0.77	0.12	0.76
(7) at functional group (C−O)	6	BEP	$y = 0.52x + 2.26$	0.29	0.55	0.87	0.66
		TSS	$y = 0.77x + 3.85$	0.36	0.55	0.71	5.68
(8) at functional group (C−OH)	6	BEP	$y = 1.22x + 1.15$	0.29	0.45	1.31	0.93
		TSS	$y = 1.16x + 0.12$	0.29	0.44	0.55	4.07
(9) small species (C−O)	8	BEP	$y = 0.95x + 1.38$	0.17	0.53	0.38	0.36
		TSS	$y = 0.91x + 1.69$	0.15	0.47	0.22	0.87
(10) small species (C−OH)	8	BEP	$y = 0.82x + 0.97$	0.18	0.49	0.55	0.54
		TSS	$y = 0.88x + 1.21$	0.17	0.44	0.21	0.76
combined C−O	14	BEP	$y = 0.70x + 1.82$	0.36	0.87	0.47	0.40
		TSS	$y = 1.11x + 0.99$	0.30	0.98	0.11	0.68
combined C−OH	14	BEP	$y = 0.78x + 1.19$	0.25	0.77	0.55	0.48
		TSS	$y = 1.09x + 0.53$	0.25	0.61	0.09	0.49
C−C scission							
(11) ring-opening	5	BEP	$y = 0.67x + 1.31$	0.45	0.74	1.70	1.93
		TSS	$y = 0.69x + 2.68$	0.43	0.84	2.02	11.08
(12) defunctionalization	10	BEP	$y = 0.81x + 0.94$	0.18	0.34	0.25	0.30
		TSS	$y = 0.82x + 2.16$	0.19	0.37	0.37	2.96
(13) small species	8	BEP	$y = 0.54x + 1.37$	0.34	0.73	1.20	0.41
		TSS	$y = 0.50x + 2.86$	0.29	0.75	0.77	2.25
combined C−C	23	BEP	$y = 0.61x + 1.27$	0.33	0.87	0.23	0.23
		TSS	$y = 0.86x + 1.81$	0.29	0.93	0.07	0.45

estimating parameters for microkinetic modeling. One approach to obtain better relations is to subdivide the data into homologous series based on the similarity of reaction families as discussed below.

Possible Homologous Series Definitions for Linear Free Energy Relations. For C−H scissions, we calculated three types of reactions (1−3 in Table 1), i.e., C−H scissions of furan ring at different degrees of ring hydrogenation, C−H scissions at various functional groups, and for comparison, C−H scissions of C2 species (CH_xCH_yR, where $x = 0 - 3$, $y = 0 - 2$, and R = H, O and OH).

C−H bond scission at the ring of F, hydrofuran (HF), dihydrofuran (DHF), trihydrofuran (TriHF) and tetrahydrofuran (THF) constitute key reactions in the furan hydrogenation to THF. We also calculated the ring C−H scissions with functional groups on the α-carbon. The fitted BEP and TSS relations are shown in Table 1. Both BEP and TSS relations have low mean AEs of 0.11 and 0.16 eV, respectively, indicating high accuracy in furanic C−H bond scission barriers. The max AEs of BEP and TSS are 0.20 and 0.40 eV, respectively.

Increasing degree of hydrogenation (furan → HF → DHF → TriHF → THF), the number of C−Pd bonds decreases (4, 3, 2, 1 and 0, respectively). Reaction energies and energy barriers were compared as a function of the degree of hydrogenation of the above species. Furan has the lowest degree of hydrogenation among them. The reaction energy and energy barrier of furan dehydrogenation are high (1.19 and 1.82 eV, respectively). The dehydrogenations of HF, DHF, TriHF and THF have low reaction energies and barriers, close to −0.5 and 1.0 eV, respectively. During dehydrogenation of F, a single hydrogen on the carbon leaves the molecule (i.e., −CH− →

dx.doi.org/10.1021/cs400942u | ACS Catal. 2014, 4, 604−612

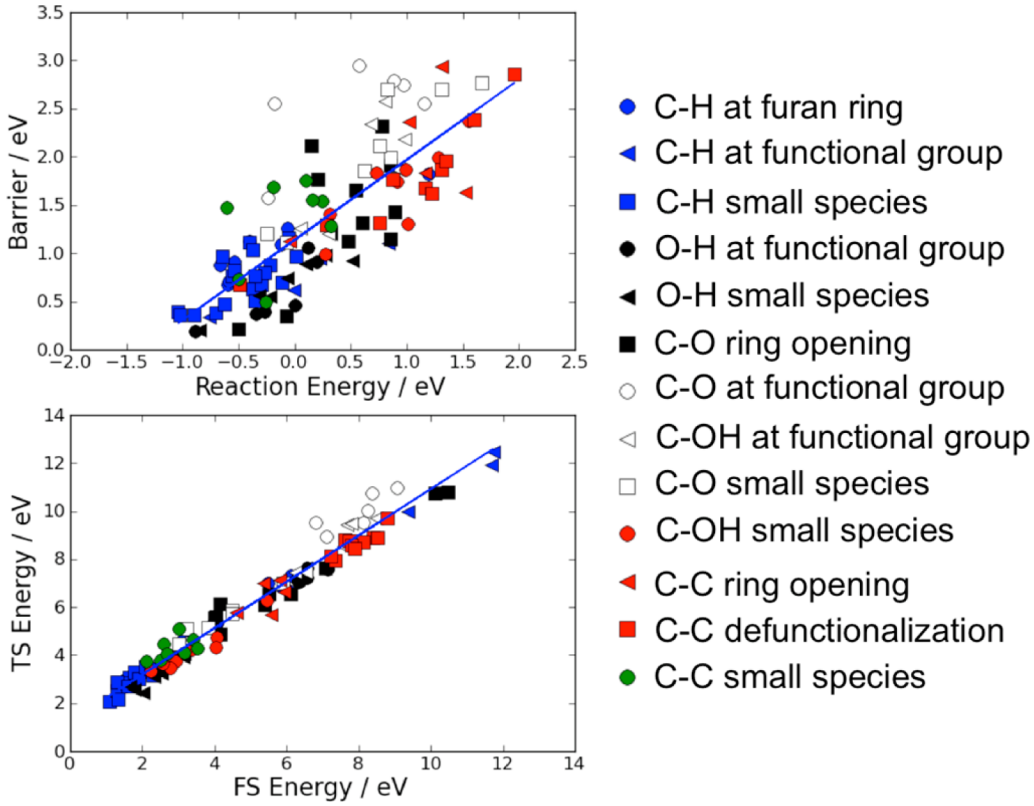

Figure 1. Universal BEP and TSS relations for all calculated reactions of furan derivatives and small molecules. See Table 1 for all reactions.

−C− + H). This is different from all other dehydrogenation reactions, in which the carbon atoms are saturated with two hydrogen atoms before dissociation ($-CH_2- \rightarrow -CH- + H$). It indicates that when dehydrogenations of species with different degrees of saturation are mixed to develop BEP and TSS relations, they lead to an offset of the data point of F dehydrogenation. Our data indicate that the AE will be lower if species with the same degree of hydrogenation were only included due to the similarity of the data set. The effect of saturation degree on the BEP relations can also be found in small molecules.[16]

Compounds in the furfural family have functional groups on the α-carbon of the furan ring of the form $-CH_xO_yH_z$. Stable species include furfural (CH_2O: $x = 2$, $y = 1$, $z = 0$), methyl furan (CH_3: $x = 3$, $y = 0$, $z = 0$), and furfuryl alcohol (CH_2OH: $x = 2$, $y = 1$, $z = 1$). We therefore tested the effect of the presence of such functional groups on furan ring hydrogenation. The data points appear to be a part of the same BEP relation of C−H scission on the furan ring regardless of whether the functional group is present or not.

BEP and TSS relations of C−H scissions at functional groups of furan derivatives have also been calculated. The mean AE and max AE of BEP relation are small (0.06 and 0.13 eV). For comparison, the mean AE and max AE of BEP of C−H bond scissions of C2 species are relatively higher (0.15 and 0.35 eV). The bigger deviations of C2 species are due to the diverse adsorption structures of these species compared to the furan derivatives. For example, on Pd(111), CCH_2OH, CH_3CH_2O, and CH_2CHOH bind via the β-carbon, the oxygen, and the α-carbon, respectively. The diversity of the adsorption structures results in different features of the transition states. Because binding of furans occurs via the four carbon atoms on the furan ring and the maximum of two atoms (C and/or O depending on the saturation degree) on functional groups, the binding structures of furan derivatives are determined from the binding preference of the furan ring. This induces similarities in the adsorption structures of furan derivatives and results in similar adsorption site and unchanged conformation in all reactions of functional groups. This explains the smaller AEs of the BEP correlations at the functional group of furanics.

BEP relations of O−H scissions of small species and at the functional group of furanics are also listed in Table 1. The BEP relation of small species has a mean AE and a max AE of 0.07 and 0.22 eV. Six data points were obtained for O−H scission of functional groups of furan derivatives, and the fitted BEP relation has a mean AE and a max AE of 0.15 and 0.27 eV. It is noticed that the fitted BEP parameters of O−H scissions of small species and at functional groups are very close. It indicates that small species and functional groups of furan derivatives share an identical O−H bond scission BEP relation. As a result, the combined BEP line has very small mean AE (0.12 eV) and max AE (0.29 eV). The statistical parameter CI was employed to analyze the equivalence of the relations at 95% confidence level. The two O−H scission BEP relations for small species and for furan derivatives are equivalent when considering the CIs of slopes and intercepts. This is in line with the analysis by AE. Therefore, one can directly apply the BEP relation from small species to estimate the barriers of O−H bond scissions of functional groups of furan derivatives.

As in Table 1, the mean AE and max AE of C−O scissions of ring-opening are 0.45 and 0.98 eV, respectively. For C−O scissions of ring-opening, the complexity of the resulting structures decreases the similarity even further, resulting in larger deviations from small molecules. The C−O and C−OH scissions at functional groups both have BEP relations with mean AEs of 0.29 eV, whereas the max AEs are 0.55 and 0.45

dx.doi.org/10.1021/cs400942u | ACS Catal. 2014, 4, 604−612

Table 2. BEP and TSS Relations of Homologous Series Based on Binding Features and Hydrogenation Degrees for Reactions of Both Furan Derivatives and C2 species, Mean and Max Absolute Errors (AE) (in eV), Confidence Intervals (CI) of Slope and Intercept

reaction	points		relation	mean AE	max AE	CI slope	CI intercept
C−O scission							
(1) Binding via C	9	BEP	$y = 0.93x + 1.34$	0.57	1.08	3.54	2.73
		TSS	$y = 0.93x + 1.88$	0.57	1.09	0.40	3.39
(2) Binding via O	4	BEP	$y = 0.46x + 2.16$	0.31	0.48	1.66	1.28
		TSS	$y = 0.39x + 6.54$	0.29	0.40	1.45	11.05
(3) Weak binding	10	BEP	$y = 1.12x + 1.06$	0.38	0.88	0.87	0.47
		TSS	$y = 0.81x + 2.08$	0.33	0.69	0.24	1.23
C−C scission							
(4) Binding via two C	10	BEP	$y = 0.84x + 1.04$	0.27	0.79	0.52	0.54
		TSS	$y = 0.80x + 2.37$	0.27	0.50	0.21	1.53
(5) Binding via one C	5	BEP	$y = 0.75x + 0.98$	0.31	0.50	0.89	1.27
		TSS	$y = 0.94x + 1.09$	0.32	0.64	0.46	3.21

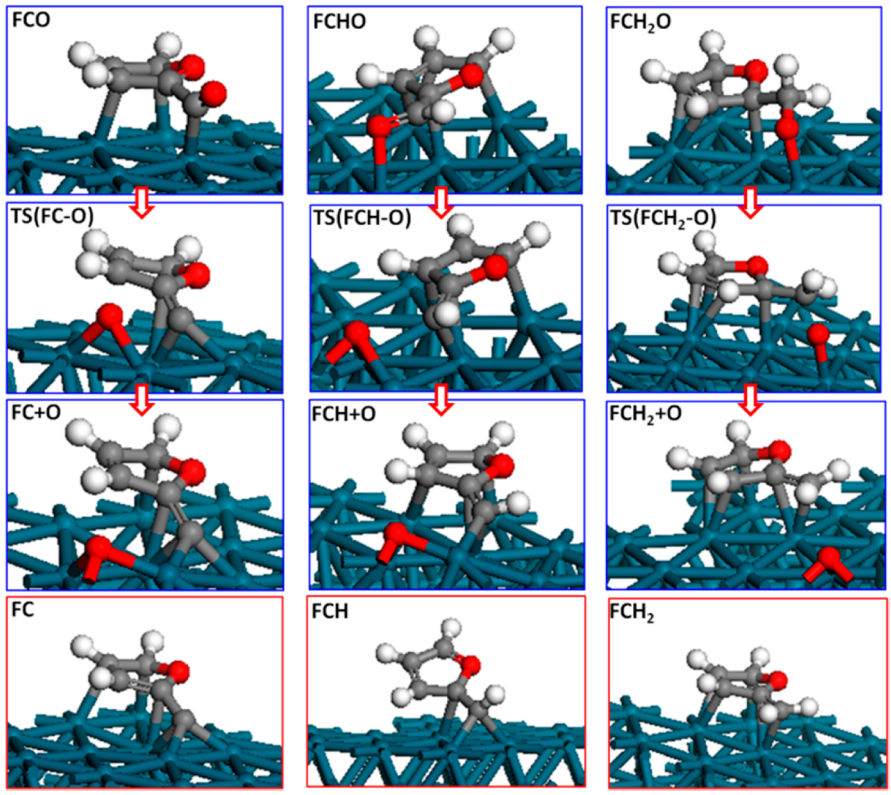

Figure 2. Structures of IS, TS and FS of C−O scissions at functional groups of $C_4H_3(CO)O$, $C_4H_3(CHO)O$ and $C_4H_3(CH_2O)O$. F stands for furan ring.

eV, respectively. The BEP relations of C−O and C−OH scissions of C2 species have mean AE of 0.17 and 0.18 eV, respectively, which are lower than those of furan derivatives.

The mean AE and max AE of C−C scissions of ring-opening are 0.45 and 0.74 eV, respectively. The C−C scissions of functional groups from the furan ring have a BEP relation with mean AE of 0.18 eV. Comparatively, the BEP relation of C−C scissions of C2 species has a mean AE of 0.34 eV, which is in between C−C ring-openings and C−C ring-side group scissions. BEP and TSS relations of C−O and C−C bond scissions show larger scatter than dehydrogenations (C−H and O−H scissions). By analyzing the CIs, all the BEP relations of C−C scissions discussed above are statistically equivalent.

Finally, we also tested new types of homologous series based on binding features. Previous works grouped the reactions into different homologous series based on the types of the molecules and bond breaking, such as C−H, O−H, C−O and C−C bonds. As discussed above, the binding of functional groups −CO, −CHO and $-CH_2O$ is different from each other. The diversity in binding features induces deviation in the BEP relations. We therefore tested the performance of BEP homologous series based on the binding features of the reacting molecules, as shown in Table 2. For example, for C−O scissions, the C and O atoms of dissociating bonds may partially bind to the surface. We therefore separated the reactions into four groups. Unfortunately, there are not enough data in each group of binding via both C and O. For the groups of binding via C, binding via O and weak binding (no C−Pd or O−Pd bond), the mean AEs of BEP relations are 0.57, 0.31 and 0.38 eV, whereas the max AEs are 1.08, 0.48 and 0.88 eV,

dx.doi.org/10.1021/cs400942u | ACS Catal. 2014, 4, 604−612

respectively. The accuracy of these homologous groups based on binding features is slightly worse or similar to the traditional ones. It has been found that C−O and C−OH bond cleavages have different BEP relations.[10] In the new homologous groups, we mixed both types of C−O cleavage reactions together, which increases scatter. The reactions at the ring and functional groups were also mixed together; this may be the other factor increasing the scatter. We expect that if the reactions were separated into more homologous groups depending on all the above factors, higher accuracy could be obtained. However, more DFT calculations will be needed to get enough data points for regression.

This paper focused on the reactions of furan derivatives on Pd(111) surface. According to previous work on small molecules, different facets, such as the (211) surface, have different BEP relations from the (111) facet.[16] For furan derivatives, we expect the BEP relations will also depend somewhat on facet.

Effect of Structure Change and Reaction Energy on the Accuracy of Linear Free Energy Relations. BEP and TSS relations rely on the similarity of the structures of transition states within a family. We find that BEP and TSS relations exist, in general, for larger molecules, and their accuracy is similar to that previously reported in literature for small molecules. The large size of furan derivatives does not worsen the performance of BEP and TSS relations of C−H and O−H scissions, because the furan ring of various derivatives strongly binds on Pd(111) with very similar structure. In contrast, the structures of adsorbed small (C2) species are more diverse with conformations varying largely with the degree of saturation of the two carbon atoms in a molecule. The deviations of C−H and C−C scission of small species are both larger than those of furan derivatives. Similarly, ring-opening (C−O and C−C scission) of the furan at different degree of hydrogenation results in considerably different ring-open structures. The diversity of structures results in larger deviations of BEP and TSS relations of C−H, C−C and C−O cleavage of ethanol species and furan ring-opening.

As shown in Figure 2, the C−O scissions at functional groups of FCO, FCHO and FCH_2O (F stands for furan ring) have different change in structure during reaction. FCO binds with the Pd(111) surface via the β and δ carbon atoms of the furan ring and the carbon atom of functional group (−CO). The transition state has both C and O of the functional group adsorbing at bridge sites. It is noted that the adsorption site of furan ring also changes from involving the β and δ carbons to involving the α and δcarbons. For the final state, the furan ring of coadsorbed FC and O has similar binding features with the transition state. However, all BEP and TSS relations were plotted with the energies of separately adsorbed FC and O (in the limit of infinite separation). The separately adsorbed FC has the furan ring binding with Pd(111) via α, γ and δ carbon atoms. The change of the binding features of the initial state, transition state and final state induces poor structural similarity between them. As a result, there is poor correlation in energy between the activation energy and the reaction energy of this reaction. This agrees with Loffreda's finding that the error of BEP was smaller when using coadsorbed reactants.[17] Figure 2 shows that the diversity in the structural change during C−C scission of FCH_2O is larger, whereas the structural change during C−C scission of FCHO is relatively small. The different degrees and different types of structural changes of the three reactions alter the correlation in energy and result in larger scatter of BEP and TSS relations.

Using smaller and more similar groups of reactions, the scatter becomes smaller due to the better structural similarity between reactions. For example, the mean AEs of the universal BEP and TSS relations are 0.34 and 0.34 eV, of the C−H bond breaking reactions are 0.18 and 0.21 eV, and of the C−H ring hydrogenation are 0.11 and 0.16 eV, respectively. In general, C−H and O−H bond breakings have smaller scatter compared to C−C and C−O bond breakings. This is in line with the degree of structural change during reaction. Dissociation of a hydrogen atom from large molecules changes their adsorption structures only slightly, whereas major structural changes usually happen upon C−C and C−O bond breaking. This is especially true for C−C and C−O ring-opening that not only affects the number of bonds with the surfaces and the bond lengths due to changing the adsorption sites but also the angles of bonds due to opening and expanding the structure of molecules. The multiple and complex changes result in large scatter in BEPs for this type of reaction.

Apart from the structure similarity, there is another important factor affecting the scatter of BEP relations. In BEP relations, the energy barriers increase with increasing reaction energies. This also means that the energy barriers of the backward reactions decrease with increasing forward reaction energies. As shown with Figure 3a,b, reactions with very negative reaction energies usually have early transition states with very small energy barriers. In this range, the energy barriers do not vary with the change of reaction energies (a slope of zero), because the transition states are structurally similar to the initial states, and have nearly no similarity with final states. In the range of intermediate reaction energies, the energy barriers increase with the increasing reaction energies with a theoretical slope usually lower than one. In the range of high reaction energies, the slope becomes one, due to having late transition states. Therefore, a BEP relation over a large range of reaction energies should exhibit three regression lines. Most reactions among the community of catalysis are in the range of intermediate reaction energies. Reactions with large reaction energies in the training set will therefore introduce large scatter of a BEP line, if a single BEP was fitted without considering the range of reaction energies. We show an example in Figure 3c.

Figure 3c shows the BEP relation for dissociation of the functional group from furan derivatives (defunctionalization). We analyze the BEP line of such C−C scissions of furan derivatives in more detail below. It is obvious that the slope in Figure 3c is close to one at large reaction energies, and this confirms the fact that the backward energy barriers do not change when they are close to zero. In this range, the transition states are very similar to the final states in structure and energy. The situation is different at intermediate reaction energies, where the transition states are intermediates between both reactants and products in most cases. In general, the transition states are more similar to reactants for negative reaction energies. Therefore, one would expect a small scatter if the BEPs were fitted within a limited range of reaction energies. The mean AE decreases from 0.18 eV (in Table 2) to 0.11 eV (in Figure 3) by narrowing the range of reaction energies that is being regressed. Unfortunately, it is currently difficult to quantitatively define the intermediate and high reaction energies due to lack of enough data.

dx.doi.org/10.1021/cs400942u | ACS Catal. 2014, 4, 604−612

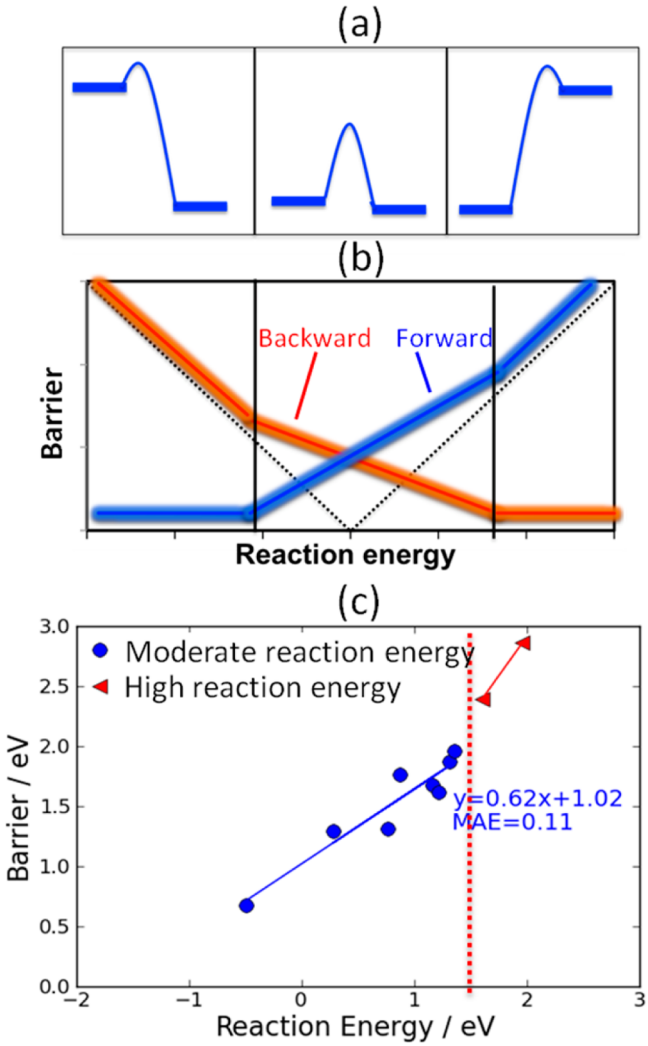

Figure 3. Schematic diagrams of BEP relations over a wide range of reaction energies. (a) IS, TS and FS for early, intermediate and late transition state cases (from left to right). (b) Corresponding barrier vs reaction energies. (c) BEP relation of C−C bond scission for cleavage of functional groups from the furan ring (defunctionalization).

Comparison of BEP Accuracy of Different Homologous Series. In this section, we carry out a general comparison of the accuracy of the different homologous series. There have obviously been a large number of BEP relations of reactions of small C1 and C2 species. The above analysis has already shown that BEP relations of small species are not exactly the same with those of the functional groups of furan derivatives. Actually, all the above four types of C−H scissions have their own BEP relation (see Table 1). In Table 1, the combined BEP relation of C−H scissions of all species mentioned above has a mean AE and a max AE of 0.18 and 0.36 eV, respectively. Whether we can directly apply small species BEP relations to biomass reactions depends on the accuracy required. A max AE of 0.36 eV may be adequate for preliminary overview of a reaction network of a complex reaction.

Figure 4 shows the mean AE and max AE of calculated energy barriers using BEP relations fitted to their own data sets, when combined BEP relations with small species, when BEP relations of small species are applied and when using the universal BEP relations, against DFT values. Using the own BEP relations, hydrogenation/dehydrogenation reactions have mean AEs of about 0.2 eV, whereas C−C and C−O scissions have larger mean AEs of about 0.4 eV. Max AEs of own BEP relations are about 0.5 eV, except for ring-openings. In contrast, the mean AE and max AE are larger (0.4 and 0.8 eV, respectively) using the universal BEP relation. C−O scissions at functional groups have a much large mean AE (1 eV) and max AE (1.5 eV), which are inadequate for computing energy profiles of this type of reaction. Moderate mean AE and max AE were obtained using the combined BEP relations (0.3 and 0.3−0.8 eV, respectively). Using BEP relations of small species, the mean AE and max AE are very similar to the respective own BEP relations, except for C−H scissions at functional groups. According to the CIs, both BEP relations of O−H scissions are equivalent, and all BEP relations of C−C scissions are equivalent. The BEP relation of C−H scissions at the furan ring is equivalent to that of small species, but the BEP relation of C−H scissions at functional groups is slightly different. This agrees with the fact that all mean AEs of BEPs of small species are close to mean AEs of their respective own BEP relations, except for the C−H scissions at functional groups (Figure 4).

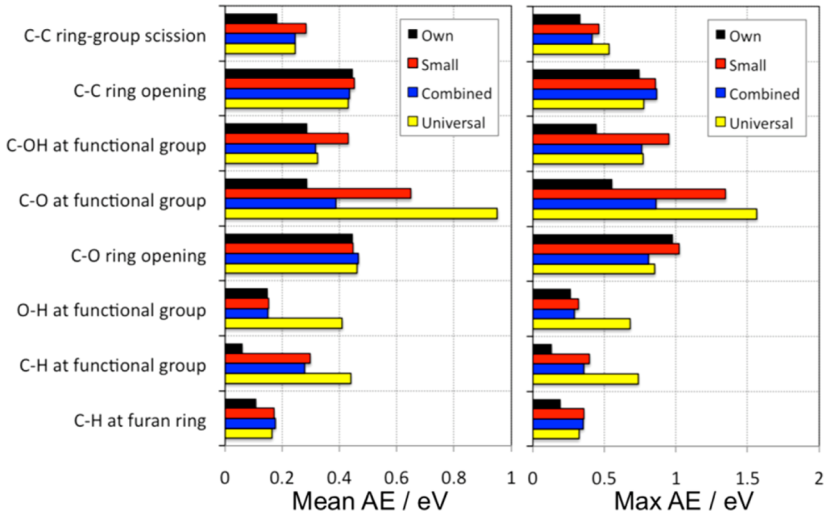

Figure 4. Mean and max absolute errors of model-predicted activation energies referred to DFT-calculated values.

dx.doi.org/10.1021/cs400942u | ACS Catal. 2014, 4, 604−612

The above analysis indicates that, in general, the accuracy of BEPs of small species and of the combined BEP relations are comparable to that of own BEPs. It is possible to employ BEP relations of small species for preliminary energy profiles, although they are not the best. For microkinetic modeling, the requirement of the accuracy depends on the sensitivity of the elementary steps. Because the performance is close to the own BEP relations (0.3 vs 0.2 eV in mean AEs), using combined BEPs or BEPs of small species is expected to be adequate for preliminary microkinetic modeling. Finally, the accuracy for calculating energy barriers of furan chemistry on Pd(111) varies as own BEPs > combined BEPs ∼ small molecule BEPs > universal BEP.

CONCLUSIONS

Using density functional theory (DFT) calculations, BEP and TSS linear free energy relations were tested for reactions of furan derivatives. It was found that BEP and TSS relations for furan derivatives perform as well as those for small (C2) species. The strong furan ring binding on Pd(111) causes similar structures for a number of reactions and, as a result, the BEPs of hydrogenation/dehydrogenation reactions show lower scatter. The structures of small oxygenated species can in fact be more diverse due to binding either via C or O, depending on which atom is unsaturated, causing larger scatter in the BEP and TSS than those of furan derivatives. The BEP and TSS relations of C−O and C−C bond scissions of furanics have larger scatter than those of small species. Hydrogenation/dehydrogenation reactions have smaller deviations compared to C−C and C−O bond breaking ones. This is in line with the degree of structural change during reaction and agrees with observations in previous works.[16,24]

Two factors have been identified to be important for accurate BEPs. The first is the range of the reaction energies. Reactions with low, intermediate, and high reaction energies possibly have early, middle, and late transition states, respectively. As a result, the BEP depends on the range of reaction energies. For low (high) reaction energies, the slope of BEPs is close to zero (one), and for intermediate reaction energies, the slope depends on both initial and final states. A BEP over a large energy range will have larger scatter. The second factor is the structural similarity. Specifically, large changes in structure between initial, transition, and final states induce poor correlation in energies and large scatter in BEPs. Grouping reactions of similar structures is expected to increase accuracy of BEPs, but more DFT data is needed to accomplish this. In general, the accuracy in calculating energy barriers of furan chemistry on Pd(111) varies as furanics individual homologous series BEPs > combined BEPs ∼ small molecule BEPs > universal BEP (see Table 1). For qualitative predictions of biomass chemistry, BEP relations of small species may be adequate.

ASSOCIATED CONTENT

Supporting Information

Further details of energies of all reactions of this paper. This material is available free of charge via the Internet at http://pubs.acs.org.

AUTHOR INFORMATION

Corresponding Author

*D. G. Vlachos. E-mail: vlachos@udel.edu.

Notes

The authors declare no competing financial interest.

ACKNOWLEDGMENTS

J.E.S. performed the small molecule calculations, assisted in the statistical analysis of the BEP and TSS correlations, and contributed to paper revision. V.V. performed part of the furan derivatives' calculations and revised the paper. S.W. performed part of the furan derivatives' calculations and wrote up the paper. D.G.V. advised the overall research and revised the paper. S.W. and D.G.V. were partially supported by the NSF-CDI grant (CMMI-0835673). V.V. acknowledges support from an NSF graduate fellowship. V.V. and J.E.S. acknowledge support from the Catalysis Center for Energy Innovation (CCEI), an Energy Frontier Research Center funded by the U.S. Department of Energy, Office of Science, Office of Basic Energy Sciences under Award Number DE-SC0001004. DFT calculations were performed in part using the TeraGrid resources provided by the Texas Advanced Computing Center (TACC) of the University of Texas at Austin.

REFERENCES

(1) Chen, Y.; Salciccioli, M.; Vlachos, D. G. *J. Phys. Chem. C* **2011**, *115*, 18707−18720.
(2) Guo, N.; Caratzoulas, S.; Doren, D. J.; Sandler, S. I.; Vlachos, D. G. *Energy Environ. Sci.* **2012**, *5*, 6703−6716.
(3) Salciccioli, M.; Stamatakis, M.; Caratzoulas, S.; Vlachos, D. G. *Chem. Eng. Sci.* **2011**, *66*, 4319−4355.
(4) Evans, M. G.; Polanyi, M. *Trans. Faraday Soc.* **1938**, *34*, 11−24.
(5) Pallassana, V.; Neurock, M. *J. Catal.* **2000**, *191*, 301−317.
(6) Liu, Z. P.; Hu, P. *J. Chem. Phys.* **2011**, *114*, 8244−8247.
(7) Logadottir, A.; Rod, T. H.; Nørskov, J. K.; Hammer, B.; Jacobsen, C. J. H. *J. Catal.* **2000**, *197*, 229−231.
(8) Nørskov, J. K.; Bligaard, T.; Logadottir, A.; Bahn, S. R.; Hansen, L. B.; Bollinger, M.; Bengaard, S. H.; Hammer, B.; Sljivancanin, Z.; Mavrikakis, M.; Xu, Y.; Dahl, S.; Jacobsen, C. J. H. *J. Catal.* **2002**, *209*, 275−278.
(9) Michaelides, A.; Liu, Z. P.; Zhang, C. J.; Alavi, A.; King, D. A.; Hu, P. *J. Am. Chem. Soc.* **2003**, *125*, 3704−3705.
(10) Sutton, J. E.; Vlachos, D. G. *ACS Catal.* **2012**, *2*, 1624−1634.
(11) Bronsted, J. N. *Chem. Rev.* **1928**, *5*, 231−338.
(12) Bell, R. P. *Proc. R. Soc. London, Ser. A* **1936**, *154*, 414−429.
(13) Van Santen, R. A.; Neurock, M.; Shetty, S. G. *Chem. Rev.* **2010**, *110*, 2005−2048.
(14) Liu, Z.; Hu, P. *J. Chem. Phys.* **2001**, *115*, 4977−4980.
(15) Alcala, R.; Mavrikakis, M.; Dumesic, J. A. *J. Catal.* **2003**, *218*, 178−190.
(16) Wang, S.; Petzold, V.; Tripkovic, V.; Kleis, J.; Howalt, J. G.; Skúlason, E.; Fernández, E. M.; Hvolbæk, B.; Jones, G.; Toftelund, A.; Falsig, H.; Bjorketun, M.; Studt, F.; Abild-Pedersen, F.; Rossmeisl, J.; Nørskov, J. K.; Bligaard, T. *Phys. Chem. Chem. Phys.* **2011**, *13*, 20760−20765.
(17) Loffreda, D.; Delbecq, F.; Vigné, F.; Sautet, P. *Angew. Chem., Int. Ed.* **2009**, *48*, 8978.
(18) Hansen, E. W.; Neurock, M. *J. Catal.* **2000**, *196*, 241−252.
(19) Linic, S.; Barteau, M. A. *J. Catal.* **2003**, *214*, 200−212.
(20) Reuter, K.; Frenkel, D.; Scheffler, M. *Phys. Rev. Lett.* **2004**, *93*, 116105.
(21) Honkala, K.; Hellman, A.; Remediakis, I. N.; Logadottir, A.; Carlsson, A.; Dahl, S.; Christensen, C. H.; Nørskov, J. K. *Science* **2005**, *307*, 555−558.
(22) Kandoi, S.; Greeley, J.; Sanchez-Castillo, M. A.; Evans, S. T.; Gokhale, A. A.; Dumesic, J. A.; Mavrikakis, M. *Top. Catal.* **2006**, *37*, 17−28.
(23) Studt, F.; Abild-Pedersen, F.; Bligaard, T.; Sørensen, R. Z.; Christensen, C. H.; Nørskov, J. K. *Science* **2008**, *320*, 1320−1322.

(24) Wang, S.; Temel, B.; Shen, J.; Jones, G.; Grabow, L. C.; Studt, F.; Bligaard, T.; Abild-Pedersen, F.; Christensen, C. H.; Nørskov, J. K. *Catal. Lett.* **2011**, *141*, 370−373.
(25) Jones, G.; Bligaard, T.; Abild-Pedersen, F.; Nørskov, J. K. *J. Phys.: Condens. Matter.* **2008**, *20*, 064239.
(26) Grabow, L. C.; Studt, F.; Abild-Pedersen, F.; Petzold, V.; Kleis, J.; Bligaard, T.; Nørskov, J. K. *Angew. Chem., Int. Ed.* **2011**, *50*, 4601−4605.
(27) Studt, F.; Abild-Pedersen, F.; Hansen, H. A.; Man, I. C.; Rossmeisl, J.; Bligaard, T. *ChemCatChem* **2010**, *2*, 98−102.
(28) Bligaard, T. *Angew. Chem., Int. Ed.* **2009**, *48*, 9782−9784.
(29) Vorotnikov, V.; Mpourmpakis, G.; Vlachos, D. G. *ACS Catal.* **2012**, *2*, 2496−2504.
(30) Xu, Y. *Top. Catal.* **2012**, *55*, 290−299.
(31) Wang, S.; Vorotnikov, V.; Vlachos, D. G. *Green Chem.* **2013**, DOI: 10.1039/c3gc41183d.
(32) Hansgen, D. A.; Vlachos, D. G.; Chen, J. G. *Nature Chem.* **2010**, *2*, 484−489.
(33) Kresse, G.; Furthmuller, J. *Comput. Mater. Sci.* **1996**, *6*, 15.
(34) Kresse, G.; Furthmuller, J. *Phys. Rev. B: Condens. Matter Mater. Phys.* **1996**, *54*, 11169.
(35) Perdew, J. P.; Burke, K.; Ernzerhof, M. *Phys. Rev. Lett.* **1996**, *77*, 3865.
(36) Grimme, S.; Antony, J.; Ehrlich, S.; Krieg, H. *J. Chem. Phys.* **2010**, *132*, 15.
(37) Blochl, P. E. *Phys. Rev. B: Condens. Matter Mater. Phys.* **1994**, *50*, 17953.
(38) Kresse, G.; Joubert, D. *Phys. Rev. B: Condens. Matter Mater. Phys.* **1999**, *59*, 1758.
(39) Monkhorst, H. J.; Pack, J. D. *Phys. Rev. B: Solid State* **1976**, *13* (12), 5188−5192.
(40) Blochl, P. E.; Jepsen, O.; Andersen, O. K. *Phys. Rev. B: Condens. Matter Mater. Phys.* **1994**, *49* (23), 16223−16233.
(41) Lamber, R.; Wetjen, S.; Jaeger, N. I. *Phys. Rev. B: Condens. Matter Mater. Phys.* **1995**, *51* (16), 10968−10971.
(42) Henkelman, G.; Uberuaga, B. P.; Jonsson, H. *J. Chem. Phys.* **2000**, *113*, 9901−9904.
(43) Sutton, J. E. Error Propagation and Uncertainty Quantification in Hierarchically Refined Microkinetic Models. Ph.D. dissertation, University of Delaware, Newark DE, 2013.
(44) Soler, J. M.; Artacho, E.; Gale, J.; García, A.; Junquera, J.; Ordejón, P.; Sánchez-Portal, D. *J. Phys.: Condens. Matter* **2002**, *14*, 2745−2779.